

DOI:10.1002/ejic.201402523

# CH<sub>3</sub>N=SF<sub>2</sub>=NCH<sub>3</sub>: Structural, Conformational, and Configurational Properties in the Gaseous and in the Condensed Phases

Norma L. Robles,<sup>[a]</sup> Simon Parsons,<sup>[b]</sup> Rüdiger Mews,<sup>[c]</sup> and Heinz Oberhammer<sup>[d]</sup>

**Keywords:** Fluorine / Sulfur / Sulfur difluoride diimides / Vibrational spectroscopy / Quantum chemistry / Conformational analysis

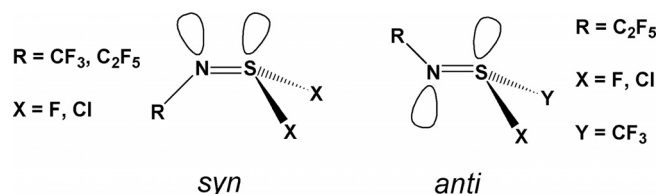
CH<sub>3</sub>–N=SF<sub>2</sub>=N–CH<sub>3</sub> (**1**) was obtained in 88 % yield from the reaction of a bis(silylated) amine RN(Si–Me<sub>3</sub>)<sub>2</sub> with a sulfur tetrafluoride imide R'N=SF<sub>4</sub> (R = R' = CH<sub>3</sub>). Single crystals suitable for X-ray crystallography were obtained by low-temperature crystallization; the data were collected at 120 K. Compound **1** crystallizes in the monoclinic space group *P*2<sub>1</sub>/*c* with *a* = 5.8356(7) Å, *b* = 12.1665(14) Å, *c* = 8.1488(8) Å, β = 110.381(7)°, *Z* = 4, in the *anti-anti* form (whereby *anti* or *syn* describe the orientation of the N–CH<sub>3</sub> bonds with respect

to opposite S=N bonds). The structural, conformational, and configurational properties of CH<sub>3</sub>–N=SF<sub>2</sub>=N–CH<sub>3</sub> were studied by vibrational spectroscopy [IR (gas) and Raman (liquid)] and quantum chemical calculations [B3LYP and MP2 with 6-311+G(2df,p) and cc-pVTZ basis sets]. Vibrational spectroscopy in the gas and liquid phases shows evidence of a configurational equilibrium of the *anti-anti* form and a slightly less favored *anti-syn* form of CH<sub>3</sub>–N=SF<sub>2</sub>=N–CH<sub>3</sub>.

## Introduction

The lack of simple, generally applicable highly efficient synthetic methods for the preparation of sulfur difluoride diimides RN=SF<sub>2</sub>=NR might be the reason why reports on the syntheses of members of this class of compounds have only been provided by three laboratories.<sup>[1]</sup> In addition to their interesting chemistry (variation of the substituents R, exchange of the sulfur-bonded fluorines, saturation of the NS bonds to give penta- and hexacoordinate species) their structural and bonding aspects are of common interest. Although sulfur nitrogen species with isolated formal double bonds [RN=SX<sub>2</sub>: CF<sub>3</sub>–N=SF<sub>2</sub>,<sup>[2]</sup> FC(O)–N=SF<sub>2</sub>,<sup>[3]</sup> C<sub>2</sub>F<sub>5</sub>–N=SF<sub>2</sub>,<sup>[4]</sup> CF<sub>3</sub>–N=SCl<sub>2</sub>,<sup>[5]</sup> FC(O)–N=SCl<sub>2</sub>,<sup>[6]</sup> C<sub>2</sub>F<sub>5</sub>–N=SCl<sub>2</sub>,<sup>[7]</sup>] and cumulated formal double bonds (RN=S=O: CF<sub>3</sub>–N=S=O,<sup>[7,8]</sup> SF<sub>5</sub>–N=S=O,<sup>[8,9]</sup> RN=S=NR: CH<sub>3</sub>–N=S=N–CH<sub>3</sub>,<sup>[10]</sup> CF<sub>3</sub>–N=S=N–CF<sub>3</sub>,<sup>[11]</sup> C<sub>2</sub>F<sub>5</sub>–N=S=N–C<sub>2</sub>F<sub>5</sub>,<sup>[11,12]</sup> and RN=SF<sub>2</sub>=O: SF<sub>5</sub>N=SF<sub>2</sub>=O<sup>[13]</sup>) have been investigated in detail, for RN=SF<sub>2</sub>=NR no reports can be found in the literature.

Especially interesting are the conformational properties of these compounds. They are dependent on the nature of the substituents bonded to sulfur and the oxidation state of the sulfur atom. For instance, considering molecules of the type CF<sub>3</sub>–N=SX<sub>2</sub><sup>[2,5]</sup> and C<sub>2</sub>F<sub>5</sub>–N=SX<sub>2</sub><sup>[4,7]</sup> (X = F, Cl), only a *syn* conformer was observed in the fluid phases (*syn* of the C–N bond with respect to the X–S–X bisector angle), whereas an equilibrium of the *anti* and *syn* forms was found for molecules of the type C<sub>2</sub>F<sub>5</sub>–N=SXY (C<sub>2</sub>F<sub>5</sub>–N=SFCF<sub>3</sub><sup>[14]</sup> and C<sub>2</sub>F<sub>5</sub>–N=SClCF<sub>3</sub><sup>[14,15]</sup>), with the *anti* form being the global minimum of the potential-energy surface (see Scheme 1). However, three stable conformations are feasible for sulfur diimides of the type R–N=S=N–R depending on the orientation of the R–N bonds with respect to opposite N=S bonds (see Scheme 2).



Scheme 1.

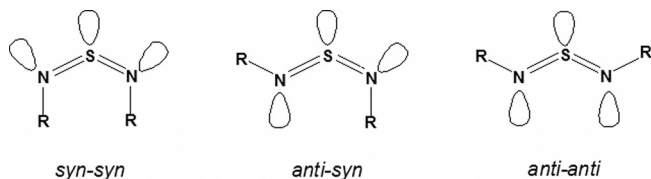
A microwave spectroscopic study of the parent compound (R = H)<sup>[16]</sup> indicated a mixture of the planar *anti-syn* and *syn-syn* conformers, whereas no existence of the *anti-anti* form was observed. For sulfur diimides that possess bulkier substituents, the *anti-syn* conformation was

[a] INQUINOA (CONICET-UNT) Instituto de Química Física, Facultad de Bioquímica, Química y Farmacia, Universidad Nacional de Tucumán, San Lorenzo 456, 4000 Tucumán, República Argentina  
E-mail: lisrobles@fbqf.unt.edu.ar  
http://www.inquinoa.org.ar/

[b] School of Chemistry and Centre for Science at Extreme Conditions  
University of Edinburgh, West Mains Road, Edinburgh, UK

[c] Institut für Anorganische und Physikalische Chemie, Universität Bremen, 28334 Bremen, Germany

[d] Institut für Physikalische und Theoretische Chemie, Universität Tübingen, 72076 Tübingen, Germany



Scheme 2.

found to be the most stable form. However, rather different equilibrium patterns were observed by gas electron diffraction for  $\text{CH}_3\text{--N=S=N--CH}_3$ <sup>[17,18]</sup> and  $\text{CF}_3\text{--N=S=N--CF}_3$ <sup>[11]</sup> whereas an *anti-anti* structure was observed for the methyl derivative, an *anti-syn/syn-syn* mixture was found for its fluorinated counterpart. Since the conformational properties of these compounds cannot be explained in terms of steric interactions, the conformational properties were rationalized on the basis of orbital interactions of sulfur and nitrogen lone pairs [lp(S) and lp(N)] with vicinal  $\sigma^*$  orbitals.<sup>[19]</sup> The *syn-syn* form possesses both N–R bonds *anti* to the sulfur lone pair and both N=S bonds *anti* to the lone pair of the opposite nitrogen atom. These orientations favor anomeric interactions of the types lp(S)  $\rightarrow$   $\sigma^*(\text{N--R})$  and lp(N)  $\rightarrow$   $\sigma^*(\text{N=S})$ , respectively. Only two such favorable *trans* arrangements are present in the *anti-syn* form and none in the *anti-anti* configuration. Although natural bond orbital (NBO) analyses<sup>[20]</sup> support the stability order *syn-syn* > *anti-syn* > *anti-anti*, the first two configurations were found to be almost equivalent in energy with a slight preference for the *anti-syn* form owing to stronger steric interactions in the *syn-syn* structure.

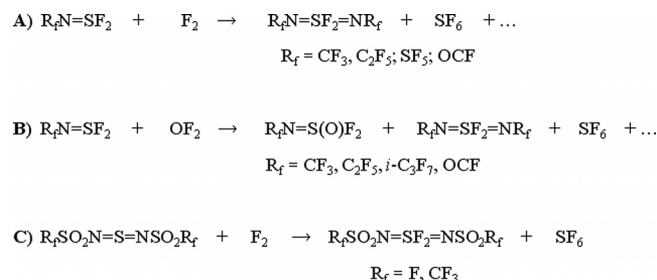
Several compounds that contain the  $\text{--N=SF}_2\text{=N--}$  group, the  $\text{S}^{\text{VI}}$  counterparts of the  $\text{--N=S=N--}$  compounds, have been prepared and characterized,<sup>[21–28]</sup> but to the best of our knowledge no attempts have been made to rationalize their properties. Here we report the X-ray structure, a vibrational analysis of the FTIR (gas) and Raman (liquid) spectra, and a quantum chemical study of  $\text{CH}_3\text{--N=SF}_2\text{=N--CH}_3$ . For this  $\text{S}^{\text{VI}}$  compound three different conformational structures are feasible (Scheme 3).

## Results and Discussion

### Synthetic Aspects

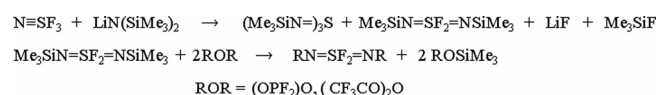
Owing to the preparative difficulties and the lack of general synthetic methods, only a small number of sulfur difluoride diimides have been reported in the literature. Lustig

and Ruff<sup>[21]</sup> isolated the first examples of this class of compounds from the fluorination of perfluoroalkyl sulfur difluoride imides, Clifford and Zeilenga<sup>[22]</sup> extended this method to  $\text{SF}_5\text{--N=SF}_2$ . Depending on the reaction conditions, in addition to the desired products, a mixture of many decomposition and byproducts are formed; yields of sulfur difluoride diimides reported from reactions on a millimolar scale range between 60% (total yield 0.6 g) for  $\text{R}=\text{CF}_3$ <sup>[21]</sup> and 8–16% (0.14 g) for  $\text{R}=\text{SF}_5$ <sup>[22]</sup> (see Scheme 4, A). Similar results were obtained when  $\text{OF}_2$  was used for the oxidative fluorination of  $\text{R--N=SF}_2$ . In addition to the products obtained from the direct fluorination,  $\text{R--N=SOF}_2$  was isolated in reasonable yields.<sup>[23]</sup> If the reaction is carefully followed (e.g., by IR spectroscopy), even  $\text{R_f--N=SF}_4$  ( $\text{R}_f = \text{C}_2\text{F}_5$ ,  $i\text{-C}_3\text{F}_7$ ) can be isolated.<sup>[24]</sup> (see Scheme 4, B). The fluorination of sulfur diimides  $(\text{R}_f\text{SO}_2\text{N=})_2\text{S}$  ( $\text{R}_f = \text{F}$ <sup>[25]</sup>,  $\text{CF}_3$ <sup>[26]</sup>) reported by Roesky et al. is a more straightforward method. The difluoride diimides were isolated in 15–25% yield; the reaction is limited to diimides with fluorine-resistant substituents in the starting materials (see Scheme 4, C). From the reaction of  $\text{N=SF}_3$  with  $\text{LiN}(\text{SiCH}_3)_2$ , Glemser and Wegener reported tris(trimethylimino)sulfur ( $\text{Me}_3\text{SiN=})_3\text{S}$  and  $\text{Me}_3\text{SiN=SF}_2\text{=NSiMe}_3$ <sup>[27]</sup> which showed for the first time that bulky groups stabilize low coordination numbers.



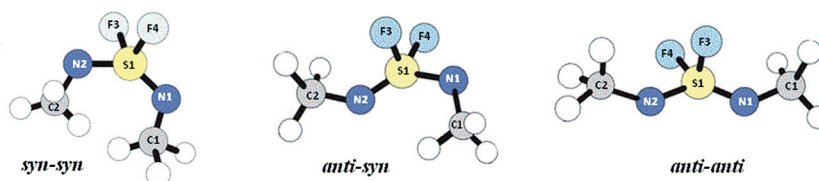
Scheme 4.

Cleavage of the Si–N bond by acid anhydrides leads to the corresponding sulfur difluoride diimides in high yields (see Scheme 5).<sup>[28]</sup>



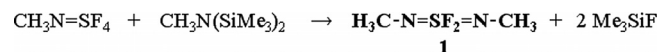
Scheme 5.

This cleavage of the Si–N bond might be widely used for high-yield preparations of new bis(imino)sulfur difluorides. The disadvantage of this method is the nontrivial prepara-



Scheme 3.

tion of the starting material. The reaction of sulfur tetrafluoride imides with primary amines or *N,N*-bis(silylated) amines, reported for the first time in this paper, is a second broadly applicable synthetic pathway to bis(imino)sulfur difluorides (see Scheme 6). The disadvantages of this method are also the problematic syntheses of the starting materials  $R-N=SF_4$ . The preparation of  $R = \text{alkyl}$ ,<sup>[26,27]</sup>  $SF_5$ ,<sup>[36]</sup>  $FSO_2$ ,<sup>[37]</sup> and  $F$ <sup>[38,39]</sup> from  $N\equiv SF_3$  as starting material is described. Perfluoroalkylsulfur tetrafluoride imides rearrange readily to pentafluorosulfur imides.<sup>[40]</sup>



Scheme 6.

At room temperature **1** is a pale yellow liquid that is not very sensitive to moisture. The influence of the oxidation state and the substituents around the sulfur center on the geometric parameters and on the conformational properties were investigated by X-ray crystallography and by NMR and IR spectroscopy, accompanied by theoretical calculations.

## Structural Investigations

Single crystals suitable for X-ray structure analysis were obtained by low-temperature crystallization on the diffractometer. The molecular structure of **1** is shown in Figure 1 and the geometric parameters are listed in Table 1 together with the calculated values. Table 2 compares experimental bond lengths and bond angles of  $CH_3-N=SF_2=N-CH_3$  (**1**) with the data of  $CH_3-N=S=N-CH_3$  (**2**)<sup>[10]</sup> (exchange of the two fluorine atoms at sulfur by a lone pair, change in the oxidation state),  $CH_3-N=S(O)F_2$  (**3**)<sup>[41]</sup> and  $O_2SF_2$  (**4**)<sup>[42]</sup> (stepwise exchange of the imino group by oxygen), and the isomer  $N\equiv SF_2-N(CH_3)_2$  (**5**)<sup>[43]</sup> (exchange of two double bonds by a triple and a single bond).

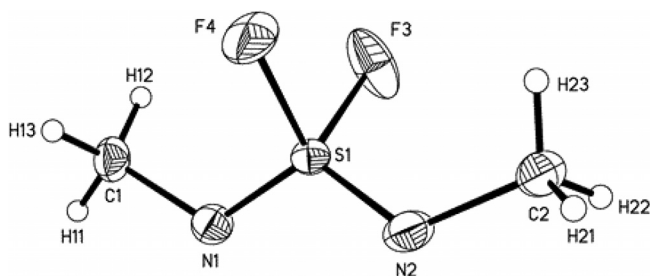


Figure 1. Molecular structure of  $H_3C-N=SF_2=N-CH_3$ . Ellipsoids enclose 30% probability surfaces.

The SN bond lengths [1.463(3) and 1.452(3) Å] in **1** are in the range expected for  $S^VI=N$  double bonds mentioned before; the  $S^VI-F$  bond lengths [1.560(2) and 1.570(2) Å] in  $S^VI=N$  derivatives seem to be only slightly influenced by co-

Table 1. Experimental and calculated geometric parameters for the *anti-anti* form of  $CH_3-N=SF_2=N-CH_3$ .<sup>[a]</sup>

	X-ray	Theoretical B3LYP/ 6-311+G(2df,p)	MP2/ cc-pVTZ
<b>Bonds</b>			
S1=N1	1.463(3)	1.479	1.487
S1=N2	1.452(3)	1.479	1.487
S1-F3(4)	1.560(2)	1.635	1.619
N1(2)-C1(2)	1.470(5)	1.462	1.466
<b>Angles</b>			
N1=S1=N2	118.8(19)	118.4	118.1
N1=S1-F3	112.0(17)	112.4	111.9
N2=S1-F3	110.9(19)	110.2	110.8
N1=S1-F4	109.8(16)	110.2	110.8
N2=S1-F4	111.8(18)	112.4	111.9
F3-S1-F4	89.8(18)	89.8	89.6
S1=N1-C1	121.1(3)	124.3	119.8
S1=N2-C2	122.9(3)	124.4	119.8
<b>Dihedral angles</b>			
N2=S1=N1-C1	168.3(3)	168.1	173.7
N1=S1=N2-C2	165.2(3)	168.1	173.7

[a] Bond lengths [Å] and angles [°]. See Figure 1 for atom numbering. Mean values are given for parameters that differ by less than their  $\sigma$  uncertainties.

Table 2. Bond lengths and bond angles of  $CH_3-N=SF_2=N-CH_3$  (**1**) and related SN/SO species.

	<b>1</b> <sup>[a]</sup>	<b>2</b> <sup>[b]</sup>	<b>3</b> <sup>[c]</sup>	<b>4</b> <sup>[d]</sup>	<b>5</b> <sup>[e]</sup>
S <sup>VI</sup> N <sup>I</sup> /S <sup>VI</sup> O <sup>I</sup>	1.463	1.532	1.454	–	1.412
S <sup>VI</sup> N <sup>II</sup> /S <sup>VI</sup> O <sup>II</sup>	1.452	1.532	1.403	1.386	1.580
S <sup>VI</sup> F <sup>I</sup>	1.560	–	1.552	1.514	1.576
S <sup>VI</sup> F <sup>II</sup>	1.570	–	1.555	1.514	1.576
N <sup>I</sup> C <sup>I</sup> /N <sup>II</sup> C <sup>I</sup>	1.470	1.464	–	–	–
N <sup>II</sup> C <sup>II</sup> /N <sup>II</sup> C <sup>II</sup>	1.469	1.464	–	–	–
N <sup>I</sup> S <sup>I</sup> N <sup>II</sup>	118.85	113.6	–	–	124.9
N <sup>I</sup> S <sup>I</sup> O <sup>II</sup>	–	–	120.65	–	–
O <sup>I</sup> S <sup>I</sup> O <sup>II</sup>	–	–	–	122.4	–
F <sup>I</sup> S <sup>I</sup> F <sup>II</sup>	89.76	–	92.35	96.6	84.8

[a] Compound **1**:  $H_3C^1N^1=S^1F^1F^2=N^2C^2H_3$ , this work. [b] Compound **2**:  $H_3C^1N^1=S^1=N^2C^2H_3$ .<sup>[17,18]</sup> [c] Compound **3**:  $H_3C^1N^1=S^1(=O^2)F^1F^2$ .<sup>[41]</sup> [d] Compound **4**:  $O^1S^1(=O^2)F^1F^2$ .<sup>[42]</sup> [e] Compound **5**:  $N^1\equiv S^1F^1F^2N^2(C^1H_3C^2H_3)$ .<sup>[43]</sup>

substituents. The large N–S–N angle [118.8(19)°] leads to a very small F–S–F angle [89.76(18)°]. Substitution of the two fluorines in **1** by a lone pair to give the diimide **2**, which changes the oxidation state of sulfur from (VI) to (IV), stretches the SN bonds from 1.46 to 1.53 Å. The N–S–N angle shrinks to 113.6°. The CN bond lengths are not affected. Exchange of the imino groups in **1** by double-bonded oxygen atoms to give **3** and **4** strengthens the bonds to the central sulfur and widens the F–S–F and the N–S–O and O–S–O angles, respectively. A completely different bonding situation is found for  $N\equiv SF_2-N(CH_3)_2$ , the isomer of **1**. The two different SN bond lengths [1.412(1) and 1.58(1) Å] are characteristic of  $S^VI=N$  triple and single bonds. Calculations [B3LYP/6-311+G(2df,p)] predict **1** to be more stable than the bond isomer **5** by  $\Delta E = 3.7$  and  $\Delta G^0 = 5.2$  kcal mol<sup>–1</sup>.

## Theoretical Calculations

The calculations predict the existence of three stable conformers, *anti-anti*, *anti-syn*, and *syn-syn*, for this S<sup>VI</sup> compound, similar to the S<sup>IV</sup> sulfur diimides. The *anti-anti* conformer possesses C<sub>2</sub> symmetry with the C–N=S=N–C chain deviating slightly from planarity (torsional angles ≈ 170°, according to both computational methods). The C–N=S=N–C chain deviates more strongly from planarity in the *anti-syn* conformer with torsional angles of 170 and –36°, and even stronger in the *syn-syn* form with both torsional angles around 40°. The relative energies and free energies of the *anti-anti* and *anti-syn* form (Table 3) are very similar. This is surprising if one considers the higher steric interactions in the *anti-syn* form. The *syn-syn* conformer lies at considerably higher energy. MP2 and B3LYP results

for the geometric parameters of the *anti-anti* conformer are given in Table 1, and vibrational frequencies of the *anti-anti* and *anti-syn* conformers in Table 4.

Table 3. Calculated relative energies and free energies [kcal mol<sup>–1</sup>]<sup>[a]</sup> and relative abundances at 298 K [%] for the *anti-anti*, *anti-syn*, and *syn-syn* conformers of CH<sub>3</sub>–N=SF<sub>2</sub>=N–CH<sub>3</sub>.

Conformer	B3LYP/ 6-311+G(2df,p)			MP2/ cc-pVTZ		
	ΔE°	ΔG°	[%]	ΔE°	ΔG°	[%]
<i>anti-anti</i>	0.00	0.00	66.3	0.00	0.00	67.5
<i>anti-syn</i>	0.64	0.41	33.7	0.30	0.44	32.4
<i>syn-syn</i>	4.59	5.11	0.0	2.82	3.83	0.1

[a] Energy differences ΔX = X(*anti-syn* or *syn-syn*) – X(*anti-anti*), (X = E°, G°).

Table 4. Experimental and calculated wavenumbers and tentative assignments of the vibrational modes for the *anti-anti* (I) and *anti-syn* (II) conformers of CH<sub>3</sub>N=SF<sub>2</sub>=NCH<sub>3</sub>.

Approximate description <sup>[a]</sup>	Experimental <sup>[b]</sup>		Theoretical <sup>[c]</sup>			
	IR (gas)	Raman (liquid)	B3LYP/6-311+G(2df,p)		MP2/cc-pVTZ	
			I	II	I	II
ν CH <sub>3</sub> sym i.p.	3003 (10)	2985 [100]	3120 (2) [20]	3117 (2) [27]	3197 (1) [24]	3192 (2) [30]
ν CH <sub>3</sub> sym o.o.p.	3003 (10)	2985 [100]	3119 (1) [31]	3115 (2) [30]	3197 (1) [28]	3191 (2) [34]
ν CH <sub>3</sub> asym i.p.	2952 (63)	2948 [40]	3084 (5) [15]	3086 (4) [16]	3158 (4) [17]	3158 (4) [15]
ν CH <sub>3</sub> asym o.o.p.	2952 (63)	2948 [40]	3084 (<1) [22]	3086 (3) [26]	3158 (<1) [17]	3158 (1) [28]
ν CH <sub>3</sub> sym i.p.	2917 (34)	2903 [35]	3027 (1) [100]	3028 (5) [100]	3077 (2) [100]	3075 (6) [100]
ν CH <sub>3</sub> sym i.p.	2917 (34)	2903 [35]	3026 (14) [2]	3026 (14) [15]	3075 (13) [2]	3074 (12) [25]
δ CH <sub>3</sub> sym i.p.	1495 sh	–	1505 (4) [<1]	1504 (3) [2]	1523 (2) [<1]	1524 (2) [3]
δ CH <sub>3</sub> sym o.o.p.	1465 (86)	1466 [14]	1504 (1) [4]	1503 (1) [3]	1522 (<1) [6]	1522 (1) [4]
δ CH <sub>3</sub> asym i.p.	1465 (86)	1460 [12]	1498 (4) [1]	1499 (4) [2]	1518 (2) [2]	1519 (4) [4]
δ CH <sub>3</sub> asym o.o.p.	1465 (86)	1450 [10]	1497 (1) [3]	1497 (2) [1]	1518 (6) [1]	1516 (2) [2]
δ CH <sub>3</sub> sym o.o.p.	1465 (86)	–	1481 (6) [3]	1480 (6) [2]	1486 (13) [2]	1486 (12) [2]
δ CH <sub>3</sub> sym i.p.	1395 sh	1435 [5]	1469 (<1) [1]	1464 (<1) [1]	1470 (<1) [<1]	1463 (<1) [1]
ν N=S o.o.p. (I)	1355 (100)	1338 [5]	1369 (100) [<1]	–	1392 (100) [<1]	–
ν N=S o.o.p. (II)	1355 (100)	–	–	1360 (100) [38]	–	1384 (100) [1]
ν N=S i.p. (II)	–	1292 [14]	1316 (2) [10]	–	1330 (2) [7]	–
ν N=S i.p. (I)	1288 (81)	1271 [24]	–	1289 (22) [9]	–	1311 (23) [7]
δ CH <sub>3</sub> sym i.p.	1171 (10)	–	1149 (<1) [1]	1149 (<1) [<1]	1154 (<1) [1]	1156 (<1) [<1]
δ CH <sub>3</sub> asym i.p.	–	1128 [4]	1146 (1) [<1]	1145 (1) [<1]	1153 (<1) [<1]	1149 (1) [1]
δ CH <sub>3</sub> asym o.o.p.	1124 (12)	1121 [4]	1144 (1) [<1]	1137 (1) [<1]	1151 (<1) [<1]	1146 (1) [<1]
δ CH <sub>3</sub> sym o.o.p.	–	1115 [4]	1132 (<1) [<1]	1136 (<1) [<1]	1137 (<1) [<1]	1142 (<1) [<1]
ν C–N o.o.p. (II)	–	–	–	932 (8) [<1]	–	972 (8) [<1]
ν C–N o.o.p. (I)	938 (47)	933 [3]	917 (<1) [<1]	–	955 (<1) [<1]	–
ν C–N i.p.	890 (97)	888 [16]	876 (31) [3]	872 (28) [2]	922 (31) [5]	915 (31) [4]
ν SF <sub>2</sub> asym (I)	763 (90)	745 [14]	–	719 (30) [4]	–	750 (37) [1]
ν SF <sub>2</sub> asym (II)	688 (76)	673 [55]	645 (30) [1]	–	692 (30) [1]	–
ν SF <sub>2</sub> sym (II)	688 (76)	673 [55]	–	637 (24) [8]	–	703 (18) [13]
ν SF <sub>2</sub> sym (I)	607 (8)	663 [58]	620 (11) [10]	–	662 (10) [11]	–
δ SF <sub>2</sub> sym wagg.	545 (14)	541 [14]	527 (2) [1]	523 (1) [1]	545 (3) [1]	542 (1) [2]
δ N=S=N	–	486 [18]	469 (<1) [1]	483 (4) [1]	485 (<1) [2]	499 (5) [1]
δ SF <sub>2</sub> asym rock.	440 (10)	435 [10]	418 (1) [1]	419 (2) [1]	435 (2) [1]	433 (3) [1]
δ SF <sub>2</sub> sym sciss.	–	400 [8]	369 (<1) [<1]	378 (2) [1]	385 (<1) [<1]	395 (2) [1]
δ SF <sub>2</sub> asym twist.	–	335 [11]	330 (<1) [1]	325 (<1) [1]	340 (<1) [1]	329 (<1) [1]
δ C–N=S o.o.p.	–	237 [13]	–	232 (1) [1]	–	239 (1) [1]
δ C–N=S o.o.p.	–	183 [13]	199 (4) [<1]	–	205 (4) [<1]	–
δ C–N=S i.p.	–	–	163 (1) [<1]	177 (2) [<1]	162 (<1) [<1]	184 (2) [1]
CH <sub>3</sub> torsion	–	85 [17]	112 (1) [<1]	108 (1) [<1]	121 (1) [<1]	110 (1) [<1]
SF <sub>2</sub> torsion	–	–	95 (<1) [<1]	99 (1) [<1]	92 (<1) [<1]	102 (<1) [<1]
CH <sub>3</sub> torsion	–	–	93 (<1) [<1]	86 (<1) [<1]	90 (<1) [<1]	89 (1) [<1]
Skeletal torsion	–	–	60 (<1) [<1]	80 (<1) [<1]	28 (<1) [<1]	85 (<1) [<1]

[a] sym: symmetric; asym: antisymmetric; i.p.: in phase; o.o.p.: out of phase; wagg.: wagging; rock.: rocking; sciss.: scissoring; twist.: twisting; sh: shoulder. [b] Relative band intensities are given in parentheses. [c] Relative IR-band intensities are given in parentheses of forms I (and II); 100%: 708 (551) and 658 (503) kmol<sup>–1</sup> with methods B3LYP and MP2, respectively. Similarly, Raman activities are given in square brackets of forms I (and II); 100%: 379 (318) and 322 (252) kmol<sup>–1</sup> with methods B3LYP and MP2, respectively.



The signals observed in the nuclear magnetic resonance spectra ( $^1\text{H}$  and  $^{19}\text{F}$  NMR) at room temperature do not demonstrate the presence of two conformers. The  $^1\text{H}$  NMR spectrum shows a single triplet signal at  $\delta = 1.97$  ppm and the  $^{19}\text{F}$  NMR spectrum shows a septet at  $\delta = 49.87$  ppm [ $J_{\text{H,F}} = 3.80$  Hz]. These spectra, however, do not exclude the presence of two conformers, they just indicate that the barrier between them is not high enough to prevent interconversion on the NMR spectroscopic timescale.

### Assignment of the Vibrational Spectra

The small energy differences predicted by the quantum chemical approximations suggests an equilibrium of two conformers in the fluid phases, which should be evidenced by a larger number of signals in the vibrational spectra. Experimental vibrational spectra registered in the gaseous (FTIR) and liquid (FT Raman) phases support the evidence for the proposed equilibrium (see Figure 2). Table 4 lists the experimental and calculated wavenumbers of  $\text{CH}_3\text{-N=SF}_2\text{-N-CH}_3$  according to different approximations [B3LYP/6-311+G(2df,p) and MP2/cc-pVTZ] as well as a tentative assignment of the  $3N - 6 = 33$  normal vibrational modes. Figures 3 and 4 show graphical comparisons between experimental and calculated infrared and Raman spectra results for the title molecule.

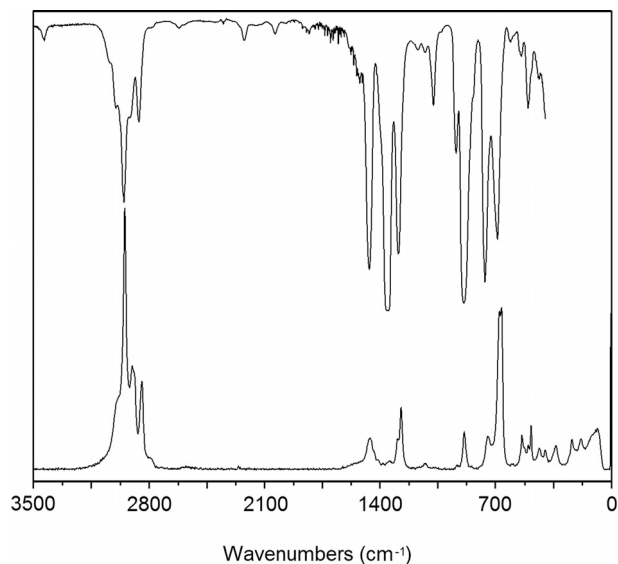


Figure 2. Vibrational spectra of  $\text{CH}_3\text{-N=SF}_2\text{-N-CH}_3$ . Upper-trace IR spectrum (gas,  $P = 2$  mbar); lower-trace Raman spectrum of a liquid sample at room temperature.

According to the predicted difference between corresponding wavenumber values for the expected conformers, only a few signals are split enough to allow an assignment to the individual conformers. Quantum chemical calculations predict strongly coupled vibrational modes for both  $\text{CH}_3$  groups in  $\text{CH}_3\text{-N=SF}_2\text{-N-CH}_3$  in either *anti-anti* or *anti-syn* configurations. These are referred to as in-phase and out-of-phase modes. The bands centered at 3003, 2952, and 2917  $\text{cm}^{-1}$  in the infrared (2985, 2948, and 2903  $\text{cm}^{-1}$ ,

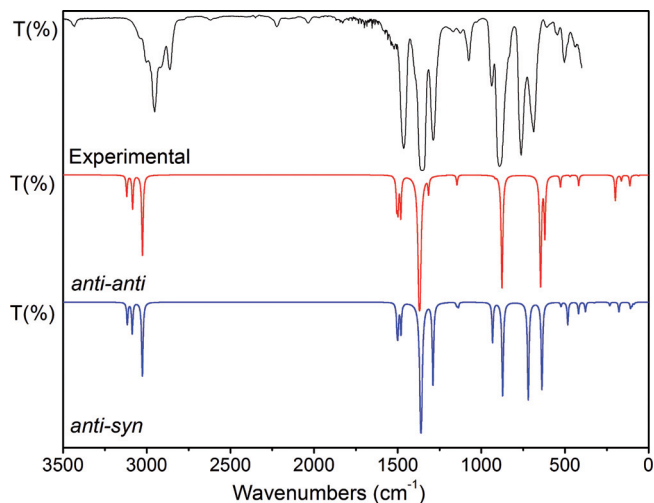


Figure 3. Graphical comparison of experimental and calculated infrared spectra of  $\text{CH}_3\text{-N=SF}_2\text{-N-CH}_3$  at the B3LYP/6-311+G(2df,p) approximation.

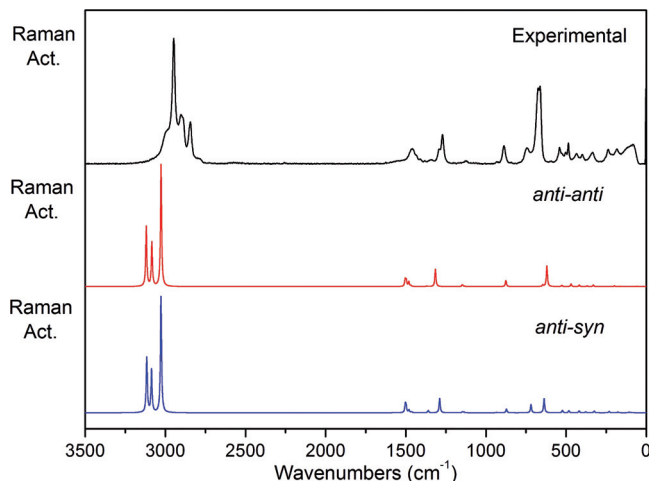


Figure 4. Graphical comparison of experimental and calculated Raman spectra of  $\text{CH}_3\text{-N=SF}_2\text{-N-CH}_3$  at the B3LYP/6-311+G(2df,p) approximation.

Raman) spectrum were assigned to the expected stretching modes of the methyl groups. This assignment is in good agreement with that reported for  $\text{CH}_3\text{-N=S(CF}_3)_2$ <sup>[44]</sup> (2994 and 2890  $\text{cm}^{-1}$  for the symmetric modes; 2937  $\text{cm}^{-1}$  for the asymmetric stretching in the infrared spectrum). The Raman spectrum allows a better assignment of the signals that belong to the bending modes of the methyl groups in the 1470–1420  $\text{cm}^{-1}$  region relative to the infrared spectrum. These spectra show only a single asymmetric signal at 1465  $\text{cm}^{-1}$  with a blueshifted shoulder at 1495  $\text{cm}^{-1}$ . An additional signal observed at 2861  $\text{cm}^{-1}$  in the infrared spectrum (2844  $\text{cm}^{-1}$ , Raman) was assigned to an overtone of the symmetric bending of the  $\text{CH}_3$  group in Fermi resonance with the asymmetric stretching of this group, as was observed in the vibrational analysis of  $\text{CH}_3\text{-N=S(CF}_3)_2$ .<sup>[44]</sup>

The two  $\text{N=S}$  stretching modes were also predicted to be strongly coupled; these are also designated as in-phase and out-of-phase. The comparison with the theoretical values

for these modes indicates that the former would be observed at lower wavenumbers. In addition, these modes are predicted to show different values for the *anti-anti* and *anti-syn* forms, which in turn allow their discrimination in the experimental spectra. The out-of-phase stretching was assigned to the band of the infrared spectrum at  $1355\text{ cm}^{-1}$  and the weak signal at  $1338\text{ cm}^{-1}$  in the Raman spectrum ( $\Delta\nu = 9$  or  $7\text{ cm}^{-1}$  according to the B3LYP and MP2 approximations, respectively). The in-phase N=S stretching was not found to account for the presence of more than one structure in the FTIR spectrum either, but the Raman spectrum did show discernible signals of medium-to-weak and weak intensity ( $1292$  and  $1271\text{ cm}^{-1}$ , respectively), which might be attributed to *anti-syn* (II) and *anti-anti* forms (I), respectively.

Two signals can be found in the C–N stretching region. The intensities of the out-of-phase modes were predicted to be very low for both conformers, although the signals observed at  $938\text{ cm}^{-1}$  in the infrared spectrum and its Raman counterpart located at  $933\text{ cm}^{-1}$  might be easily assigned to the *anti-anti* conformer (form I in Table 5). However, both in-phase stretches were assigned to the strong infrared signal at  $890\text{ cm}^{-1}$  ( $888\text{ cm}^{-1}$ , Raman). It is clear that the assignment proposed for the signals in the C–N stretching region and those in the N=S frequency range is consistent with an equilibrium between both predicted forms.

Table 5. Crystal data and structure refinement for  $\text{CH}_3\text{--N=SF}_2\text{=N--CH}_3$ .

Empirical formula	$\text{C}_2\text{H}_6\text{F}_2\text{N}_2\text{S}$
$M_r$	128.15
$D_{\text{calcd.}} [\text{Mg m}^{-3}]$	1.569
$F(000)$	264
$T [\text{K}]$	120(2)
Crystal size [mm]	$1.50 \times 1.00 \times 1.00$
Crystal description	colorless cylinder
$\lambda [\text{\AA}]$	0.71073
Crystal system	monoclinic
Space group	$P2_1/c$
$a [\text{\AA}]$	5.8356(7)
$b [\text{\AA}]$	12.1665(14)
$c [\text{\AA}]$	8.1488(8)
$\alpha [^\circ]$	90
$\beta [^\circ]$	110.381(7)
$\gamma [^\circ]$	90
$V [\text{\AA}^3]$	542.34(11)
$Z$	4
Cell measurement reflections used	3134
Cell measurement $\theta_{\text{min./max.}} [^\circ]$	3.149–25.018
Index ranges	$-6 \leq h \leq 6, 0 \leq k \leq 14, 0 \leq l \leq 9$
$\mu [\text{mm}^{-1}]$	0.517
Reflections collected	4304
Independent reflections [ $R_{\text{int}} = 0.056$ ]	954
Goodness-of-fit on $F^2$	1.0517
Largest diff. peak/hole [ $\text{e \AA}^{-3}$ ]	0.58/–0.33

More convincing proof of this equilibrium might be derived from the  $\text{SF}_2$  stretching region. The three signals found in the vibrational spectra were assigned to four stretching modes: the strong band at  $763\text{ cm}^{-1}$  in the infrared spectrum ( $745\text{ cm}^{-1}$ , Raman) belongs to the *anti-syn* asymmetric stretching; a single infrared feature centered at

$688\text{ cm}^{-1}$  ( $673\text{ cm}^{-1}$ , Raman) would account for the *anti-syn* symmetric and *anti-anti* asymmetric stretching modes. Finally, the medium-intensity Raman signal at  $663\text{ cm}^{-1}$  ( $607\text{ cm}^{-1}$ , IR) can be attributed to the *anti-anti*  $\text{SF}_2$  symmetric stretch.

### Bonding and Conformation in Sulfur Difluoride Diimides

As mentioned above, sulfur diimides  $\text{R--N=S=N--R}$  with  $\text{R} = \text{H}$  and  $\text{CF}_3$  exist in the gas phase as mixtures of sterically unfavorable *anti-syn* and *syn-syn* conformers. According to quantum chemical calculations, the sterically most favorable *anti-anti* form is much higher in energy. These unexpected conformational properties have been rationalized for  $\text{CF}_3\text{--N=S=N--CF}_3$  on the basis of an NBO analysis.<sup>[19]</sup> According to this analysis of the B3LYP/6-311+G(df) wavefunction orbital, interactions (anomeric effects) of the S lone pair with  $\sigma^*(\text{N--C})$  orbitals and of the N lone pairs with vicinal  $\sigma^*(\text{S=N})$  bonds stabilize the sterically most unfavorable *syn-syn* conformer by  $55\text{ kcal mol}^{-1}$ . Such orbital interactions are much lower for the *anti-syn* conformer ( $22\text{ kcal mol}^{-1}$ ) and even less for the *anti-anti* form ( $8\text{ kcal mol}^{-1}$ ). Thus, the strong anomeric effects in the *syn-syn* and *syn-anti* conformers override the steric repulsion in these structures.

The conformational properties of  $\text{CH}_3\text{--N=SF}_2\text{=N--CH}_3$  differ strongly from those of the related  $\text{S}^{\text{IV}}$  compound  $\text{CH}_3\text{--N=S=N--CH}_3$ . According to vibrational spectra and quantum chemical calculations, the  $\text{S}^{\text{VI}}$  compound exists in the gas and liquid phases as a mixture of the sterically most favorable *anti-anti* and the less favorable *anti-syn* conformer. On the basis of the experimental vibrational spectra it is not possible to derive an accurate ratio for the conformational mixture, since calculated IR intensities and Raman activities are also rather unreliable. However, the very similar 2:1 ratio of *anti-anti/anti-syn* predicted by both computational methods (B3LYP and MP2) is in agreement with the experimental spectra. The sterically unfavorable *syn-syn* form is much higher in energy according to quantum chemical calculations (see Table 3). The different conformational properties of  $\text{S}^{\text{IV}}$  and  $\text{S}^{\text{VI}}$  compounds are due to strongly different orbital interactions. Since the  $\text{S}^{\text{VI}}$  atom does not possess an electron lone pair, only interactions of the N lone pairs with  $\sigma^*(\text{S--F})$ ,  $\sigma^*(\text{S=N})$ , and  $\pi^*(\text{S=N})$  orbitals can occur (see Figure 5).

NBO analyses of the B3LYP/6-311++G(2df,p) wavefunctions result in rather similar orbital interaction energies for the three conformers,  $36\text{ kcal mol}^{-1}$  for *anti-anti*,  $43\text{ kcal mol}^{-1}$  for *anti-syn*, and  $39\text{ kcal mol}^{-1}$  for *syn-syn*. These orbital interaction energies explain the similar contributions of the *anti-anti* form and the sterically less favorable *anti-syn* structure, which possesses slightly higher stabilization energies.

The  $\text{S}^{\text{IV}}$  and  $\text{S}^{\text{VI}}$  compounds also possess different structural properties. According to microwave (MW) and gas-phase electron-diffraction (GED) experimental data and quantum chemical calculations, all three conformers of R–

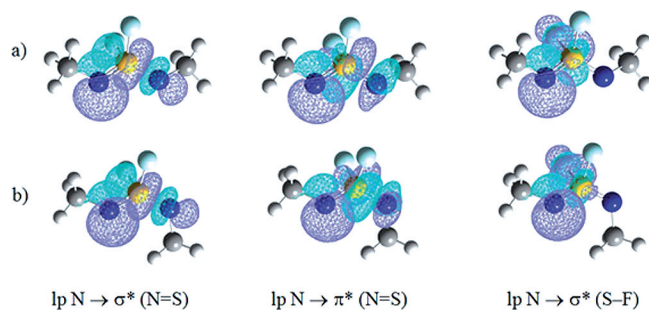


Figure 5. NBO orbitals [B3LYP/6-311+G(2df,p)] for relevant orbital interactions in the (a) *anti-anti* and (b) *anti-syn* conformers of  $\text{CH}_3\text{-N=SF}_2\text{=N-CH}_3$ .

$\text{N=S=N-R}$  compounds with  $\text{R} = \text{H}$ ,  $\text{CH}_3$ , and  $\text{CF}_3$  possess planar  $\text{C-N=S=N-C}$  skeletons. By contrast, quantum chemical calculations for  $\text{CH}_3\text{-N=SF}_2\text{=N-CH}_3$  predict nonplanar structures for the  $\text{C-N=S=N-C}$  group in all three conformers (see above).

## Conclusion

$\text{CH}_3\text{-N=SF}_2\text{=N-CH}_3$  was prepared in high yield from the corresponding sulfur tetrafluoride imide  $\text{CH}_3\text{-N=SF}_4$  and the bis(silylated) amine  $\text{H}_3\text{C-N(SiMe}_3)_2$ . We expect that the reaction of sulfur tetrafluoride imides with primary amines or bis(silylated) derivatives thereof provide a general, high-yield synthetic pathway to bis(imino)sulfur difluorides  $\text{RN=SF}_2\text{=NR'}$ .

The applied quantum chemical methods are a powerful tool for the investigation of the structural and conformational properties of the title molecule; they predict three stable conformers with *anti-anti*, *anti-syn*, and *syn-syn* configurations of the  $\text{C-N=S=N-C}$  entity. From this set, only the *anti-anti* structure was found in the solid state by X-ray structure determination. According to the predicted energy difference between *anti-anti* and *anti-syn* conformers (mean value for  $\Delta G^\circ = 0.42 \text{ kcal mol}^{-1}$ ), both forms are expected to be observed in the experimental vibrational spectra of the fluid phases. The vibrational spectra do not allow an accurate determination of the ratio of the two conformers but are in agreement with the *anti-anti/anti-syn* ratio of about 2:1, which is predicted by the MP2 and B3LYP calculations.

## Experimental Section

**Materials and Methods:**  $[(\text{CH}_3)_3\text{Si}]_2\text{N-CH}_3$ <sup>[29]</sup> and  $\text{CH}_3\text{-N=SF}_4$ <sup>[30,31]</sup> were prepared according to the literature methods. The NMR spectra were recorded with a Bruker-E 60, and the mass spectra were recorded with a Varian MAT CH-5 spectrometer. Gas infrared spectra were registered with an FT-Bruker IFS 85 and FT-Bruker IFS 66v spectrometer in the  $4000\text{--}400 \text{ cm}^{-1}$  region ( $P = 2 \text{ mbar}$ ); Raman spectra of liquid samples held in glass capillaries were performed in the  $4000\text{--}50 \text{ cm}^{-1}$  region with an FT-Bruker IFS 85 and FT-Bruker RFS 100/S spectrometer equipped with an Nd:YAG 150 mW laser. Elemental analyses were performed at Mikroanalytisches Labor Beller, Göttingen.

**Preparation of  $\text{CH}_3\text{-N=SF}_2\text{=N-CH}_3$ :** Under vacuum  $[(\text{CH}_3)_3\text{Si}]_2\text{N-CH}_3$  (3.00 g, 17.9 mmol) and  $\text{CH}_3\text{-N=SF}_4$  (2.57 g, 18.4 mmol) were condensed at  $-196^\circ\text{C}$  into a 300 mL glass vessel equipped with a Teflon valve. The mixture was continuously stirred for 48 h at  $60^\circ\text{C}$  and then purified by repeated trap-to-trap vacuum condensations at  $-196$ ,  $-70$ , and  $-60^\circ\text{C}$ . The trap at  $-60^\circ\text{C}$  held 1.93 g (15.1 mmol)  $\text{CH}_3\text{-N=SF}_2\text{=N-CH}_3$  (yield: 88.7%). The slightly yellow liquid was stable at room temperature in the absence of moisture. It boiled at  $95^\circ\text{C}$  and solidified to colorless crystals at  $-102^\circ\text{C}$ .  $^1\text{H}$  NMR ( $\text{SO}_2$  as solvent) [ $\text{Si}(\text{CH}_3)_4$  external]:  $\delta = 1.97$  (tr,  $J = 3.80 \text{ Hz}$ ) ppm;  $^{19}\text{F}$  ( $\text{CFCl}_3$  internal):  $\delta = 49.87$  (sept) ppm. MS (EI,  $70 \text{ eV}$ ):  $m/z$  (%) = 128 (100)  $[\text{M}]^+$ , 127 (88)  $[\text{M} - \text{H}]^+$ ; 108 (9.4)  $[\text{M} - \text{HF}]^+$ , and further fragments.  $\text{C}_2\text{H}_6\text{F}_2\text{N}_2\text{S}$  (128.14): calcd. C 18.75, H 4.69, F 29.69, N 21.87, S 25.00; found C 18.9, H 4.74, F 29.6, N 21.7, S 25.1.

**Crystallographic Analysis:** A sample of  $\text{CH}_3\text{-N=SF}_2\text{=N-CH}_3$  contained in a glass capillary was mounted on a Bruker APEX diffractometer equipped with an Oxford Cryosystem low-temperature device. A solid-liquid equilibrium was established in the sample at 170.6 K, and a crystal was obtained by cooling the sample at a rate of  $360 \text{ K h}^{-1}$  to 165 K. The sample was then cooled to 120 K for data collection. Data were collected with Mo- $K_\alpha$  radiation and integrated to  $2\theta = 50^\circ$ . A correction for systematic errors was applied using SADABS.<sup>[32]</sup> The structure was solved by Patterson methods (DIRDIF)<sup>[33]</sup> and refined by full-matrix least-squares against  $|F|^2$  (CRYSTALS)<sup>[34]</sup> with hydrogen atoms located in a difference map and refined with bond lengths and angles restrained to typical values. All non-hydrogen atoms were modeled with anisotropic displacement parameters. A listing of crystal and refinement parameters is given in Table 5.

CCDC-962496 contains the supplementary crystallographic data for this paper. These data can be obtained free of charge from The Cambridge Crystallographic Data Centre via [www.ccdc.cam.ac.uk/data\\_request/cif](http://www.ccdc.cam.ac.uk/data_request/cif).

**Computational Methods:** The geometric structures, conformational properties and vibrational frequencies of  $\text{CH}_3\text{-N=SF}_2\text{=N-CH}_3$  were studied with the B3LYP/6-311+G(2df,p) and MP2/cc-pVTZ methods by using the Gaussian 03 program system.<sup>[35]</sup>

## Acknowledgments

Financial support by the German Volkswagen Stiftung (I/78 724), the Deutscher Akademischer Austauschdienst (DAAD), and Engineering and Physical Sciences Research Council (EPSRC), United Kingdom is gratefully acknowledged. The Argentinian authors also acknowledge Consejo Nacional de Investigaciones Científicas y Técnicas (CONICET) and Universidad Nacional de Tucumán (UNT). Specially thanks are expressed to Prof. Dr. H. Willner (University of Wuppertal) for recording the Raman spectra.  $\text{CH}_3\text{N=SF}_2\text{=NCH}_3$  was first reported by Reiner Bartsch in his diploma thesis, Göttingen, Germany (R. Mews, R. Bartsch, 1980, unpublished results).

- [1] M. Lustig, J. K. Ruff, Redstone Research Laboratories, Huntsville, Alabama, USA; A. F. Clifford, Department of Chemistry, Polytec Institute, Virginia, Blacksburg, Virginia, USA; O. Glemser, H. W. Roesky, R. Mews, University of Göttingen, Germany.
- [2] a) J. E. Griffiths, D. F. Sturman, *Spectrochim. Acta A* **1969**, 23A, 1355; b) F. Trautner, D. Christen, R. Mews, H. Oberhammer, *J. Mol. Struct.* **2000**, 525, 135; c) N. L. Robles, E. H. Cutin, C. O. Della Védova, *J. Mol. Struct.* **2006**, 784, 265.



- [3] a) A. F. Clifford, C. S. Kobayashi, *Inorg. Chem.* **1965**, 4, 571; b) Álvarez, R. M. S. Cutin, E. H. R. M. Romano, C. O. Della Védova, *Spectrochim. Acta Part A* **1996**, 52, 667; c) Leibold, C. E. H. Cutin, C. O. Della Védova, H.-G. Mack, R. Mews, H. Oberhammer, *J. Mol. Struct.* **1996**, 375, 207.
- [4] a) Smith, W. C. C. W. Tullock, R. D. Smith, V. A. Engelhardt, *J. Am. Chem. Soc.* **1959**, 81, 3165; b) Robles, N. L. E. H. Cutin, R. Mews, C. O. Della Védova, *J. Mol. Struct.* **2010**, 978, 131.
- [5] a) Haist, R. E. H. Cutin, C. O. Della Védova, H. Oberhammer, *J. Mol. Struct.* **1999**, 475, 273; b) Álvarez, R. M. S. Cutin, E. H. R. M. Romano, C. O. Della Védova, *Spectrochim. Acta* **1999**, 552A, 615.
- [6] a) H. W. Roesky, R. Mews, *Angew. Chem. Int. Ed. Engl.* **1968**, 7, 217; b) Leibold, C. R. M. S. Álvarez, E. H. Cutin, C. O. Della Védova, H. Oberhammer, *Inorg. Chem.* **2003**, 42, 4071.
- [7] a) M. Lustig, *Inorg. Chem.* **1966**, 5, 1317; b) N. L. Robles, R. M. S. Álvarez, E. H. Cutin, C. O. Della Védova, M. F. Erben, R. Boese, H. Willner, R. Mews, *Eur. J. Inorg. Chem.* **2007**, 3535.
- [8] A. Flores Antognini, H. Oberhammer, E. H. Cutin, N. L. Robles, *J. Mol. Struct.* **2012**, 1023, 75.
- [9] P. Kricke, I. Stahl, R. Mews, O. Glemser, *Chem. Ber.* **1981**, 114, 3467.
- [10] a) B. Cohen, A. G. MacDiarmid, *Angew. Chem. Int. Ed. Engl.* **1963**, 2, 151; *Angew. Chem.* **1963**, 75, 207; b) B. Cohen, A. G. MacDiarmid, *J. Chem. Soc. A* **1966**, 1780.
- [11] I. L. Knunyants, Ya. F. Komissarou, B. L. Dyatkin, L. T. Lantseua, *Izv. Akad. Nauk SSSR, Ser. Khim.* **1973**, 4, 943; *Chem. Abstr.* **1975**, 79, 42635.
- [12] W. Leidinger, W. Sundermeyer, *Chem. Ber.* **1982**, 115, 2892.
- [13] a) R. Höfer, O. Glemser, *Z. Naturforsch. B* **1975**, 30, 458; b) Álvarez, R. M. S. Cutin, E. H. R. Mews, H. Oberhammer, *J. Phys. Chem. A* **2007**, 111, 2243.
- [14] a) I. Stahl, R. Mews, O. Glemser, *Z. Naturforsch. B* **1978**, 33, 1417; b) N. L. Robles, H. Oberhammer, R. Mews, E. H. Cutin, *Spectrochim. Acta Part A* **2014**, 125, 1.
- [15] N. L. Robles, D. M. Chemes, H. Oberhammer, R. Mews, E. H. Cutin, *article to be published*.
- [16] S. L. Hinchley, P. Trickey, H. E. Robertson, B. A. Smart, D. W. H. Rankin, D. Leusser, B. Walford, D. Stalke, M. Buehl, S. J. Obrey, *J. Chem. Soc., Dalton Trans.* **2002**, 4607.
- [17] J. Kuyper, P. H. Isselmann, F. C. Mijlhoff, A. Spelbos, G. Rennes, *J. Mol. Struct.* **1975**, 29, 247.
- [18] H. M. Tuononen, R. J. Suontamo, J. U. Valkonen, R. S. Laitinen, T. Chivers, *Inorg. Chem.* **2003**, 42, 2447.
- [19] R. Haist, R. Mews, H. Oberhammer, *Mendeleev Commun.* **2006**, 1.
- [20] A. E. Reed, L. A. Curtis, F. Weinhold, *Chem. Rev.* **1988**, 88, 899.
- [21] M. Lustig, J. K. Ruff, *Inorg. Chem.* **1965**, 4, 1444.
- [22] A. F. Clifford, G. R. Zeilenga, *Inorg. Chem.* **1969**, 8, 1789.
- [23] a) I. Stahl, R. Mews, O. Glemser, *J. Fluorine Chem.* **1976**, 7, 55; b) I. Stahl, R. Mews, O. Glemser, *Chem. Ber.* **1977**, 110, 2398.
- [24] I. Stahl, R. Mews, O. Glemser, *Angew. Chem. Int. Ed. Engl.* **1980**, 19, 408; *Angew. Chem.* **1980**, 92, 393.
- [25] H. W. Roesky, D. P. Babb, *Angew. Chem. Int. Ed. Engl.* **1969**, 8, 674; *Angew. Chem.* **1969**, 81, 705.
- [26] H. W. Roesky, G. Holtschneider, *Z. Anorg. Allg. Chem.* **1970**, 378, 168.
- [27] O. Glemser, J. Wegener, *Angew. Chem. Int. Ed. Engl.* **1970**, 9, 309; *Angew. Chem.* **1970**, 82, 324.
- [28] O. Glemser, J. Wegener, R. Höfer, *Chem. Ber.* **1972**, 105, 474.
- [29] R. C. Osthoff, S. W. Kantor, *Inorg. Synth.* **1957**, 5, 55.
- [30] a) R. Bartsch, H. Henle, Th. Meier, R. Mews, *Chem. Ber.* **1988**, 121, 451; b) R. Mews, *Angew. Chem. Int. Ed. Engl.* **1978**, 17, 530; *Angew. Chem.* **1978**, 90, 561.
- [31] A. G. Iriarte, E. H. Cutin, R. M. S. Álvarez, R. Mews, H. Oberhammer, *J. Mol. Struct.* **2009**, 919, 343.
- [32] G. M. Sheldrick, *SADABS*, version 2008/1, University of Göttingen, Germany, **2008**.
- [33] P. T. Beurskens, G. Beurskens, W. P. Bosman, R. de Gelder, R. S. Garcia-Granda, R. O. Gould, R. Israel, J. M. M. Smits, *The DIRDIF96 Program System*, Technical Report of the Crystallography Laboratory, University of Nijmegen, the Netherlands. **1996**.
- [34] P. W. Betteridge, J. R. Carruthers, R. I. Cooper, K. Prout, D. J. Watkin, *J. Appl. Crystallogr.* **2003**, 36, 1487.
- [35] M. J. Frisch, G. W. Trucks, H. B. Schlegel, G. E. Scuseria, M. A. Robb, J. R. Cheeseman, J. Montgomery Jr., A. T. Vreven, K. N. Kudin, J. C. Burant, J. M. Millam, S. S. Iyengar, J. Tomasi, V. Barone, B. Mennucci, M. Cossi, G. Scalmani, N. Rega, G. A. Petersson, H. Nakatsuji, M. Hada, M. Ehara, K. Toyota, R. Fukuda, J. Hasegawa, M. Ishida, T. Nakajima, Y. Honda, O. Kitao, H. Nakai, M. Klene, X. Li, J. E. Knox, H. P. Hratchian, J. B. Cross, V. Bakken, C. Adamo, J. Jaramillo, R. Gomperts, R. E. Stratmann, O. Yazyev, A. J. Austin, R. Cammi, C. Pomelli, J. W. Ochterski, P. Y. Ayala, K. Morokuma, G. A. Voth, P. Salvador, J. J. Dannenberg, V. G. Zakrzewski, S. Dapprich, A. D. Daniels, M. C. Strain, O. Farkas, D. K. Malick, A. D. Rabuck, K. Raghavachari, J. B. Foresman, J. V. Ortiz, Q. Cui, A. G. Baboul, S. Clifford, J. Cioslowski, B. B. Stefanov, G. Liu, A. Liashenko, P. Piskorz, I. Komaromi, R. L. Martin, D. J. Fox, T. Keith, M. A. Al-Laham, C. Y. Peng, A. Nanayakkara, M. Challacombe, P. M. W. Gill, B. Johnson, W. Chen, M. W. Wong, C. Gonzalez, J. A. Pople, *Gaussian 03*, revision E.01, Gaussian, Inc., Wallingford, CT, **2007**.
- [36] A. Waterfeld, R. Mews, *Angew. Chem. Int. Ed. Engl.* **1982**, 21, 354.
- [37] Th. Meier, R. Mews, *J. Fluorine Chem.* **1989**, 42, 81.
- [38] D. D. Des Marteau, K. Seppelt, *Angew. Chem. Int. Ed. Engl.* **1980**, 19, 643.
- [39] D. D. Des Marteau, H. H. Eysel, H. Oberhammer, H. Günther, *Inorg. Chem.* **1982**, 21, 1607.
- [40] C. W. Tullock, D. Coffman, D. Muetterties, *J. Am. Chem. Soc.* **1964**, 86, 357.
- [41] S. Parsons, R. Mews, *article to be published*.
- [42] D. Mootz, A. Merschenz-Quack, *Acta Crystallogr., Sect. C* **1988**, 44, 924.
- [43] T. Borrmann, E. Lork, R. Mews, S. Parsons, J. Petersen, W.-D. Stohrer, P. G. Watson, *Inorg. Chim. Acta* **2008**, 361, 479.
- [44] F. Trautner, R. M. S. Álvarez, E. H. Cutin, N. L. Robles, R. Mews, H. Oberhammer, *Inorg. Chem.* **2005**, 44, 7590.

Received: June 10, 2014

Published Online: September 8, 2014